ACTA
PROTOZOOLOGICA

Acta Protozool. (2015) 54: 171–182
www.ejournals.eu/Acta-Protozoologica
doi:10.4467/16890027AP.15.014.3211

Morphological and Morphogenetic Redescriptions and SSU rRNA Gene-based Phylogeny of the Poorly-known Species *Euplotes amieti* Dragesco, 1970 (Ciliophora, Euplotida)

Mingjian LIU[1], Yangbo FAN[1], Miao MIAO[2], Xiaozhong HU[1], Khaled A. S. AL-RASHEID[3], Saleh A. AL-FARRAJ[3], Honggang MA[1]

[1] Laboratory of Protozoology, Institute of Evolution & Marine Biodiversity, Ocean University of China, Qingdao 266003, China; [2] College of Life Sciences, University of Chinese Academy of Sciences, Beijing 100049, China; [3] Zoology Department, College of Science, King Saud University, Riyadh 11451, Saudi Arabia

Abstract. This paper investigates the morphology and morphogenesis during binary fission of a Chinese population of *Euplotes amieti* Dragesco, 1970, a fresh water form which has previously not been well defined. This organism is morphologically very similar to the well-known *Euplotes eurystomus* but differs from the latter both in the number of dorsal kineties and the molecular data. According to the information obtained, it is characterized by a combination of features including nine frontoventral cirri, ca. 60 membranelles, 12–15 dorsal kineties, a macronucleus in the shape of the number 3, and a 'double-*eurystomus*' type of silverline system. Its morphogenesis proceeds broadly in the same pattern as in its congeners. In this study, the SSU rRNA gene was sequenced for the first time, and phylogenetic analyses indicated that it is closely related to the *eurystomus-aediculatus-woodruffi-* complex. Considering the extreme similarities in morphology between *E. amieti* and *E. eurystomus*, we believe that the four sequences (four isolates) under the name of *Euplotes eurystomus* (No. FR873716; FR873717; EF193250; AJ310491 deposited in GenBank) are very likely from misidentified material; that is, they represent different populations of *Euplotes amieti*.

Key words: Euplotidae, fresh water ciliate, ontogenesis, phylogenetic analysis, taxonomy.

INTRODUCTION

The ciliate family Euplotidae is one of the most complicated and confused taxa with a huge variety of species, worldwide distribution and strong adaptability in marine, freshwater and terrestrial biotopes (Tuffrau 1960, Carter 1972, Curds and Wu 1983, Song *et al.* 2009). With the improvement in impregnation methods during the last few decades, some new and poorly known euplotids have been discovered and well-defined (Pan *et al.* 2012, Chen *et al.* 2013, Jiang *et al.* 2013). Borror and Hill (1995) split *Euplotes* into four genera: *Euplotes*, *Euplotopsis*, *Euplotoides*, and *Moneuplotes* based on characteristics of cortical structure, endosymbionts, morphometric data, morphoge-

Address for correspondence: Honggang Ma, Laboratory of Protozoology, Institute of Evolution and Marine Biodiversity, Ocean University of China, Qingdao 266003, China; E-mail: mahg@ouc.edu.cn; Miao Miao, College of Life Sciences, University of Chinese Academy of Sciences, Beijing 100049, China; E-mail: doublemiao@126.com

netic patterns and ecology. This classification scheme has been questioned, however, by some of the phylogenetic research of the family Euplotidae (Petroni *et al*. 2002, Schwarz *et al*. 2007, Achilles-Day *et al*. 2008, Yi *et al*. 2009, 2012). In 2009, Yi *et al*. grouped species of Euplotidae into five well-supported clades based on a combination of morphological and phylogenetic information from Petroni *et al*. (2002) and Schwarz *et al*. (2007). The results showed that *Euplotopsis*, *Euplotoides* and *Moneuplotes* occupied derived positions in all phylogenetic trees and were mixed with species of other genera in their respective clades (Yi *et al*. 2009). The phylogenetically derived research, therefore, failed to support any of the subdivisions of the *Euplotes* s. l. proposed by previous investigators (Curds 1975, Gates and Curds 1979, Borror and Hill 1995). In the present paper, we support the notion of *Euplotes*, *Euplotopsis*, *Euplotoides*, and *Moneuplotes* being remerged back into a single genus *Euplotes*.

Euplotes amieti was originally described by Dragesco (1970) and shares many characteristics with *Euplotes eurystomus*, except its larger body size and greater number of dorsal kineties. Dragesco redescribed a Chadian population in 1972, while Curds (1975) and Dragesco and Dragesco-Kernéis (1986) also each mentioned the type population of *Euplotes amieti*. In 2003, Dragesco isolated *Euplotes amieti* in Rwanda and redescribed it as *Euplotoides amieti*. Although *Euplotes amieti* has been described three times by Dragesco, there are still no detailed illustrations and photomicrographs available of the morphology of *in vivo* and protargol-impregnated specimens, and this species has not previously been recorded in Asia. Additionally, the morphogenetic process has not yet been studied. In the present paper we provide a comprehensive redescription of *Euplotes amieti* based on morphologic and morphogenetic data and we also document its morphogenesis during cell division. Small subunit ribosomal RNA (SSU rRNA) gene sequence data are also supplied, and the phylogenetic position in the SSU rRNA gene tree is determined.

MATERIALS AND METHODS

Cells origin: The Chinese population of *Euplotes amieti* was originally isolated in October 2004 from fresh waters in Shanghai, China, with the culture then being kept in store in the Laboratory of Protozoology at the East China Normal University. A strain acquired from Dr. Hong Zeng, Fujian Normal University was used in the current studies.

Morphology and morphogenesis: The specimens were examined *in vivo* using bright field and Nomarski differential interference contrast microscopy at 100–1000 × (Fan *et al*. 2014). The protargol impregnation method of Wilbert (1975) was used in order to reveal the infraciliature and nuclear apparatus. The Chatton-Lwoff silver nitrate method was used to reveal the silverline systems (Foissner 2014). Counts and measurements of impregnated specimens were performed with an ocular micrometer. Drawings were made with the help of a camera lucida (Shao *et al*. 2013a). To illustrate the changes occurring during the morphogenetic process, parental cirri are depicted with contour lines, whereas new ones are shaded black (Shao *et al*. 2013b). Terminology is mainly according to Curds (1975).

DNA extraction, PCR amplification and sequencing: Genomic DNA extraction, PCR amplification, and sequencing of the SSU rRNA gene were performed according to Huang *et al*. (2014). Two primers: 18S-F (5'-AACCTGGTTGATCCTGCCAGT-3') and 18S-R (5'-TGATCCTTCTGCAGGTTCACCTAC-3') (modified from Medlin *et al*. 1988) were used for SSU rRNA gene amplification. Cycling parameters for PCR amplifications were as follows: 5 min initial denaturation (94°C), followed by 30 cycles of 30 s at 94°C, 30 s at 58°C, and 1 min 15 s at 72°C, with a final extension of 10 min at 72°C. In order to minimize sequence errors, the high fidelity TaKaRa Ex Taq (TaKaRa, Otsu, Japan) was used for PCR amplification.

Phylogenetic analyses: A total of 74 taxa were obtained from the NCBI/GenBank databases for phylogenetic analyses, including all the isolates of *Euplotes eurystomus*. *Protocruzia adherens* (AY217727) and *Protocruzia contrax* (DQ190467) were selected as the out-group species. Sequences were aligned with MUSCLE v3.7 (Edgar 2004) with default parameters. Resulting alignments were refined by trimming the sequences at both ends, and these were then further edited visually using BioEdit 7.0.5.2 (Hall 1999), yielding an alignment of 1840 characters.

Bayesian inference (BI) analysis was performed using the CIPRES Science Gateway (The CIPRES Portals. URL: http://www.phylo.org/sub_sections/portal) with MrBayes v.3.2.2 on XSEDE (Ronquist and Huelsenbeck 2003, Pratas *et al.* 2009, Pfeiffer and Stamatakis 2010) using the GTR+I (=0.2678)+G (=0.5615) evolutionary model as the most suitable model selected by MrModeltest v.2 (Nylander 2004) according to the Akaike Information Criterion (AIC) for Bayesian inference (BI). Markov chain Monte Carlo (MCMC) simulations were then run with two sets of four chains using the default settings: i.e. a chain length of 1,000,000 generations, with a sample frequency of 100. After discarding a 25% burn in, all the remaining trees were used to calculate the posterior probability using a majority rule consensus. Maximum likelihood (ML) analyses were carried out online on the CIPRES Science Gateway (The CIPRES Portals. URL: http://www.phylo.org/sub_sections/portal) with RAxML-HPC2 on XSEDE (7.6.3) (Stamatakis 2006, Stamatakis *et al*. 2008) using the GTR+I+G evolutionary model as the best model according to the AIC criterion selected by the program Modeltest v.3.4 (Posada and Crandall 1998). Node Support came from 1000 bootstrap replicates. TreeView v.1.6.6 (Page 1996) and MEGA 4.0 (Tamura *et al*. 2007) were used to visualize tree topology. Phylogenetic trees were constructed according to Huang *et al.* (2012). Systematic classification is mainly according to Lynn (2008).

RESULTS

Class Spirotrichea Bütschli, 1889
Order Euplotida Small & Lynn, 1985
Genus *Euplotes* Ehrenberg, 1830
***Euplotes amieti* Dragesco, 1970 (Figs 1 and 2; Table 1)**

Since this species has never been clearly diagnosed before, we present here an improved diagnosis based on the original description, the African populations and the Chinese population.

Improved diagnosis: Fresh water *Euplotes*, about 130–240 μm × 70–160 μm *in vivo*; buccal field prominent and broad, triangular in outline, about 1/2 to 2/3 of body length with about 52–70 membranelles; invariably nine frontoventral, five transverse and two left marginal cirri, usually two caudal cirri; 12–15 dorsal kineties with about 18–32 dikinetids in mid-dorsal row; macronucleus typically in the shape of the number three (hereafter, 3-shaped); dorsal silverline system double-*eurystomus* type.

Description of Shanghai population: Cells *in vivo* about 130–200 μm × 70–100 μm, generally asymmetric oval in outline; anterior end slightly rounded while posterior end often widely rounded (Figs 2A, B). Cell body dorsoventrally flattened about 2 : 1 with dorsal side a little arched and ventral side concave (Fig. 2D). Buccal field broad and triangular in outline, approximately 1/2–2/3 of body length (Figs 2A, B). A conspicuous collar positioned at anterior end of dorsal side (Figs 2A, B). No ridges on dorsal side, but four short, inconspicuous ridges between transverse cirri on ventral side (Fig. 1A). Numerous irregular ellipsoid to oval granules (possibly mitochondria) about 1.5–2 μm across, extremely densely packed beneath dorsal and ventral pellicle (Fig. 2F); about nine bar-shaped granules, ca. 1 μm long, densely packed around dorsal cilia beneath pellicle. Cytoplasm colorless, highly transparent at marginal area, and containing several to many different-sized lipid droplets and several food vacuoles (1.5–2 μm in diameter) in central part (Figs 1A, 2B). One contractile vacuole 25–30 μm in diameter, adjacent to the rightmost transverse cirrus (Figs 1A, 2A); pulsating at intervals of 1–2 min. Locomotion typically by moderately fast crawling or slight jerking.

Adoral zone prominent, composed of 60–65 membranelles, commencing at anterior part of frontoventral cirri on ventral side with ca. five membranelles, extending to collar zone on dorsal side with ca. 16 membranelles. Other membranelles extending from collar zone to ventral side with about a 90-degree curve and occupying 1/2–2/3 body length in a sigmoidal shape

Table 1. Morphometric data of *Euplotes amieti* Dragesco, 1970.

Characteristics	Max	Min	Mean	SD	CV	n
Body length	165	122	142.50	10.27	7.2	25
Body width	114	78	97.20	8.89	9.1	25
Length of buccal field	100	87	94.64	4.21	4.5	25
Length of buccal field: body length	0.74	0.59	0.67	0.05	7.7	25
Length of paroral membrane	24	17	20.44	1.53	7.5	25
Width of paroral membrane	4	3	3.60	0.50	13.9	25
Number of adoral membranelles	65	60	61.80	2.25	3.6	25
Number of dorsal kineties	14	12	13.10	0.46	3.5	39
Number of frontoventral cirri	9	9	9.00	0	0	25
Number of transverse cirri	5	5	5.00	0	0	25
Number of marginal cirri	2	2	2.00	0	0	25
Number of caudal cirri	3	2	2.10	0.27	13.0	39
Number of dikinetids in mid-dorsal kinety	26	18	21.80	1.78	8.2	25
Number of dikinetids in leftmost dorsal kinety	20	11	17.00	2.14	12.6	25

Data are based on protargol-impregnated specimens. Measurements in μm. CV, coefficient of variation in %; Max, maximum; Mean, arithmetic mean; Min, minimum; n, number of cells measured; SD, standard deviation.

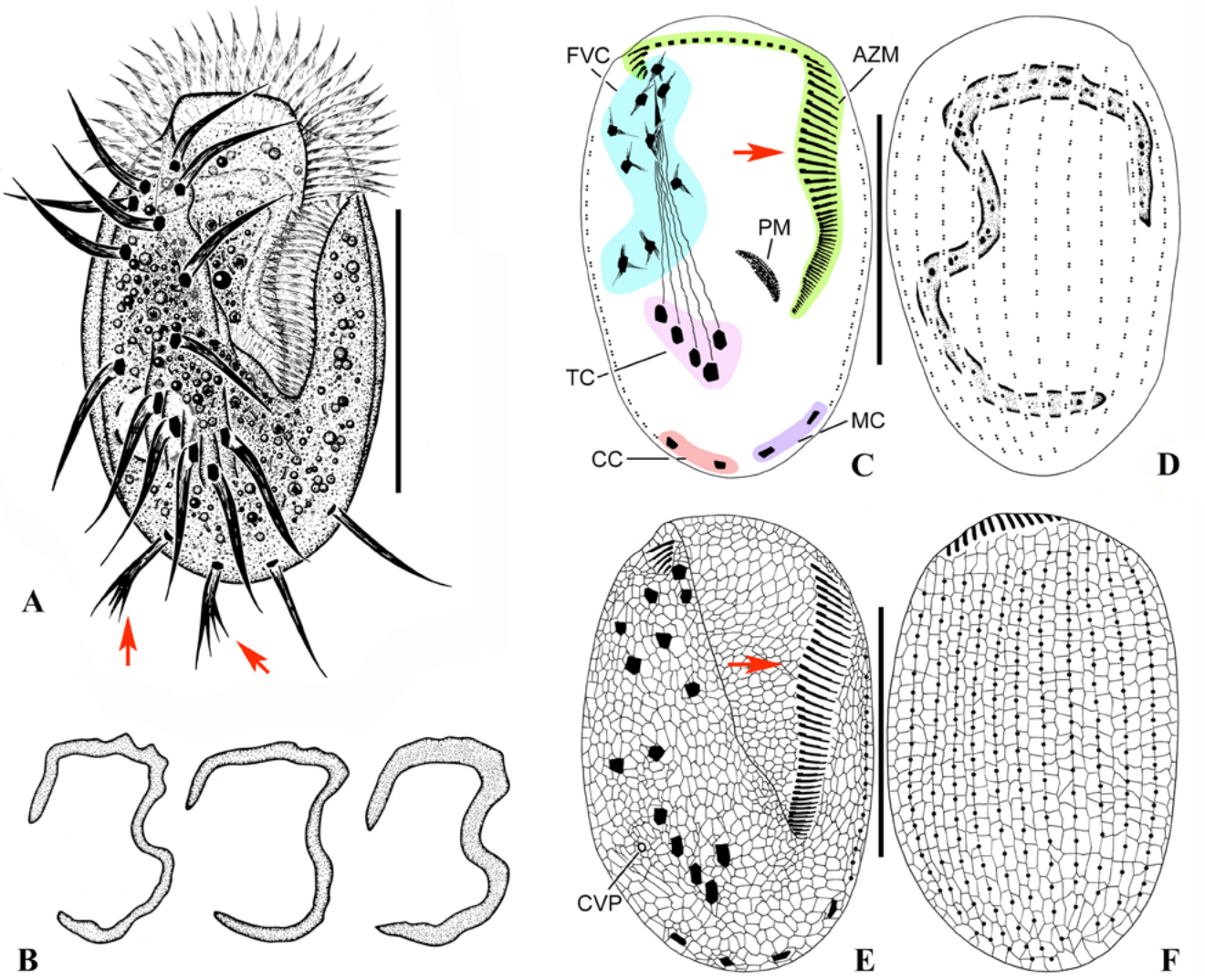

Fig. 1. *Euplotes amieti* Dragesco, 1970 *in vivo* (A), after protargol (B–D) and silver nitrate (E, F) impregnation. (**A**) Ventral view of a representative cell. Arrows indicate caudal cirri. (**B**) Different shapes of macronucleus. (**C, D**) Ventral (C) and dorsal (D) view, showing the infraciliature and nuclear apparatus. Arrow shows the sigmoidal adoral zone. (**E, F**) Silverline system on ventral (E) and dorsal side (F). Arrow shows the sigmoidal adoral zone. AZM, adoral zone of membranelles; CC, caudal cirri; CVP, contractile vacuole pore; FVC, frontoventral cirri; MC, marginal cirri; PM, paroral membrane; TC, transverse cirri. Scale bars: 100 μm.

(Figs 1A, C, E, 2A, J, K). Paroral membrane about 20 μm × 4 μm, composed of many irregularly arranged kinetosomes, positioned below buccal lip, and extending right to the proximal end of the adoral zone (Fig. 2J); cilia of paroral membrane about 6 μm long. Consistently nine frontoventral cirri (ca. 35 μm long), five transverse cirri (ca. 45 μm long), and two left marginal cirri (ca. 35 μm long) (Figs 1C, 2J); usually two caudal cirri, occasionally three, ca. 30 μm long (Fig. 2I). 12–14 (usually 13) dorsal kineties with dikinetids extending almost entire length of body (four out of 39 specimens analyzed possessed 12 dorsal kineties and another four had 14). Usually 10–12 kinety rows located on dorsal side. Mid-dorsal kinety with 21–24 dikinetids (Fig. 1D). Macronucleus 3-shaped, with many small spherical nucleoli (Figs 1D, 2J, K); one micronucleus, round to oval, located in the anterior part of the body near the left side, generally set in a distinct depression of

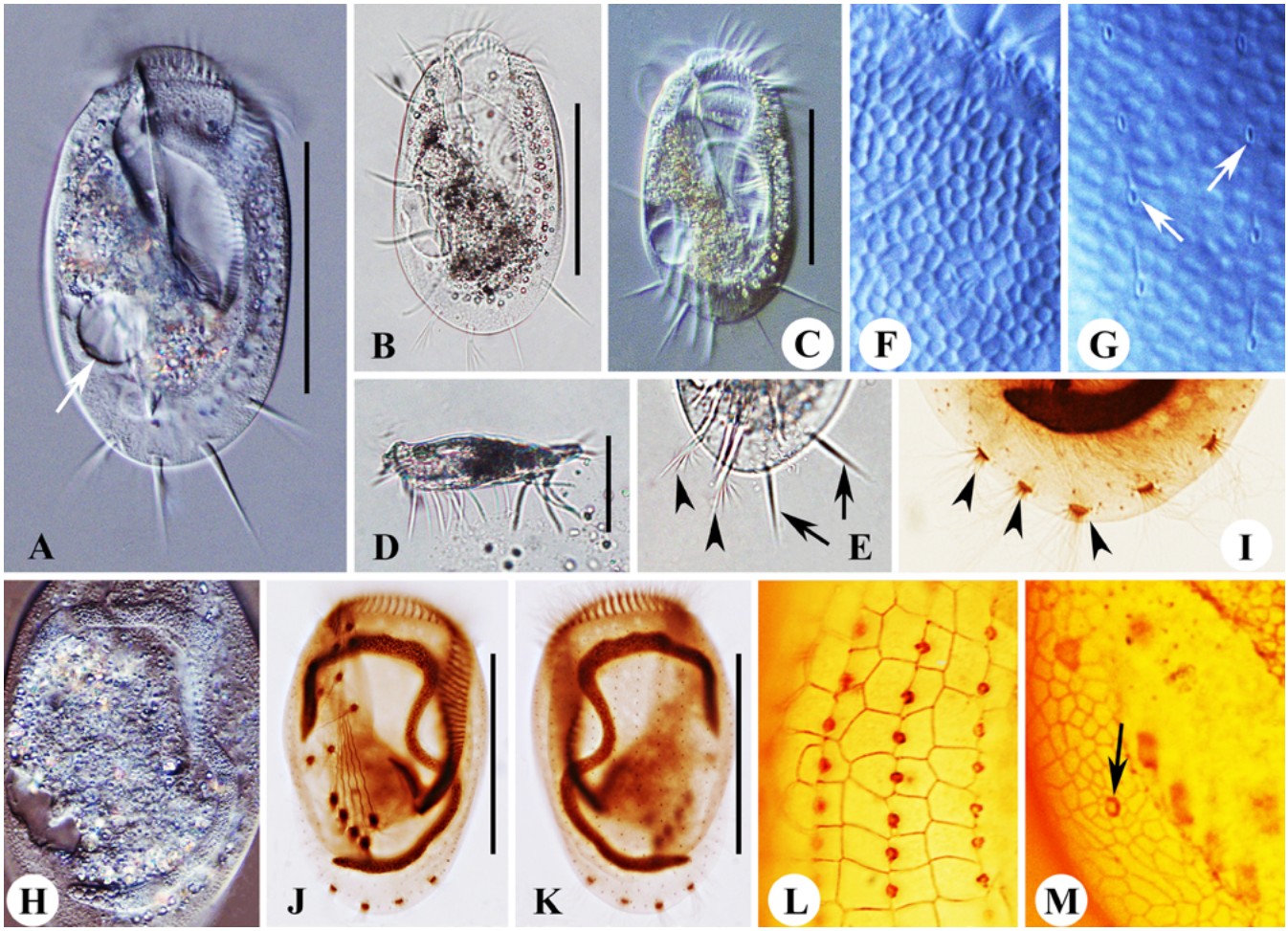

Fig. 2. Photomicrographs of *Euplotes amieti* Dragesco, 1970 *in vivo* (A–H), after protargol (I–K) and silver nitrate (L, M) impregnation. (**A**) Ventral view of a representative individual. Arrow points to the contractile vacuole. (**B, C**) Different body shapes. (**D**) Lateral view showing flattened body. (**E**) Posterior part of an individual, arrowheads show the caudal cirri and arrows indicate the left marginal cirri. (**F**) Numerous irregular ellipsoid to oval granules (possibly mitochondria) extremely densely packed beneath dorsal and ventral pellicle. (**G**) Detailed view, arrows point to the basal positions of dorsal cilia. (**H**) Showing the endoplasm and the typical 3-shaped macronucleus. (**I**) Individual with three caudal cirri (arrowheads). (**J, K**) Ventral (J) and dorsal (K) view of the same specimen, showing the infraciliature and nuclear apparatus. (**L, M**) Portion of dorsal (L) and ventral (M) silverline system. Arrow indicates the position of contractile vacuole pore. Scale bars: 100 μm.

the macronucleus. Silverline system on dorsal side of the double-*eurystomus* type (Figs 1E, F, 2L). One contractile vacuole pore positioned in the right part of the transverse cirri on ventral side (Fig. 1E).

Morphogenesis (Figs 3 and 4): Stomatogenesis starts with the appearance of a small patch of kinetosomes, which is the opisthe's oral primordium, within a pouch beneath the cortex of the ventral surface, positioned between the cytostome and the left marginal cirri (Figs 3A, 4C). As the pouch enlarges, kinetosomes proliferate rapidly and begin to align into membranelles from the anterior end and organize towards the posterior (Figs 3C, 4E).

An additional anlage, the primordium for the paroral membrane (UM-anlage), appears within the subcortical pouch, which is located close to the posterior end of the oral primordium (Figs 3C, 4E).

Following this, the UM-anlage begins to lengthen and becomes broader. Throughout the entire morphogenetic process, the parental adoral zone remains nearly intact (Figs 3C, E, 4E).

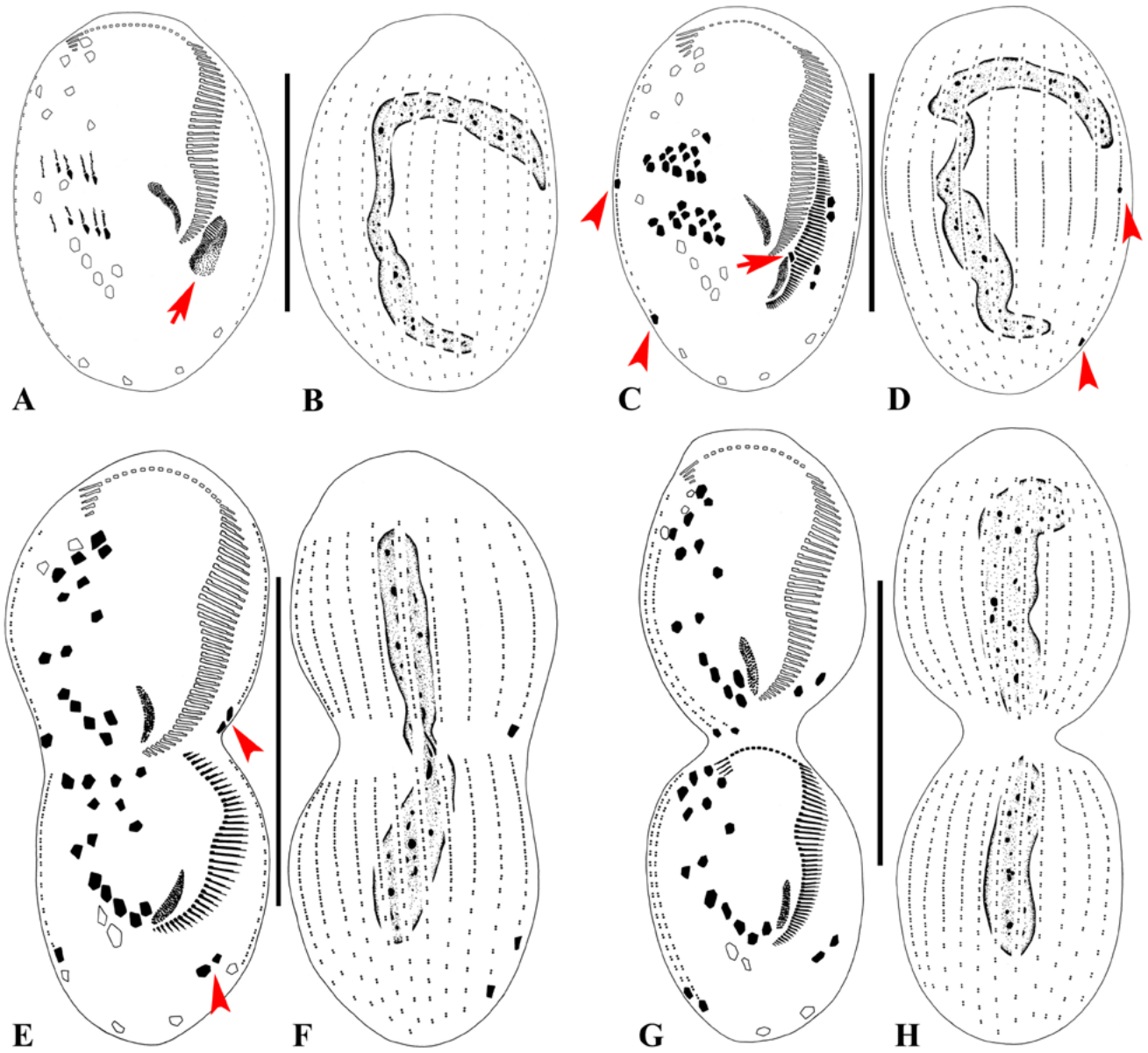

Fig. 3. Morphogenesis of *Euplotes amieti* after protargol impregnation. (**A, B**) Ventral (A) and dorsal (B) view of the same specimen at an early stage to show the five frontal-ventral-transverse cirral streaks and oral primordium within which membranelles are forming (arrow). (**C, D**) Ventral (C) and dorsal (D) view of the same specimen at a middle stage to show the completion of the cirral formation, the differentiation of caudal cirri at posterior ends of the two rightmost dorsal anlagen (arrowheads), the *de novo* formation of the new marginal cirri and the frontal cirrus I/1 in both proter and opisthe (arrows). (**E, F**) Ventral (E) and dorsal (F) view, showing the migration of newly formed cirri and the development of dorsal kineties, arrowheads show the marginal cirri. (**G, H**) Ventral (G) and dorsal (H) side of the same divider at a late stage showing infraciliature and nuclear apparatus. Scale bars: A–D = 100 μm; E–H = 150 μm.

Development of frontal-ventral-transverse cirral anlagen (FVT-anlagen): at the same time as the oral primordium is formed, two sets of FVT-anlagen develop *de novo* as multiple basal bodies anterior to the transverse cirri (Figs 3A, 4B); each set consists of five streaks (anlagen II–VI). Each cirral streak extends in both directions with a proliferation of kinetosomes. Obviously, no parental ciliary organelles are involved in the formation of these anlagen. The cirral streaks then broaden and break apart in a 3:3:3:2:2

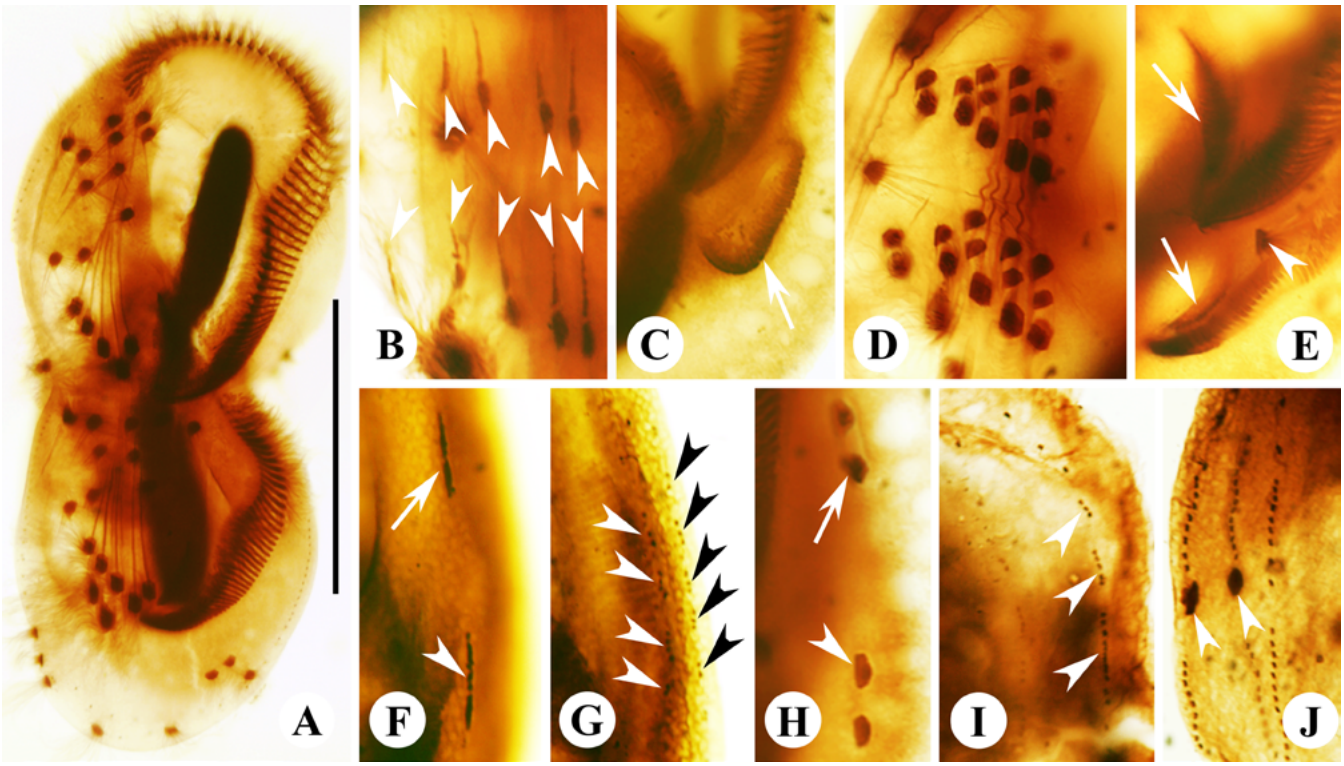

Fig. 4. Photomicrographs of *Euplotes amieti* during morphogenesis after protargol impregnation. (**A**) Ventral view of a middle divider showing the migration of cirri and the division of the macronucleus. (**B, C**) Ventral view of an early divider demonstrating two sets of frontal-ventral-transverse cirral streaks (arrowheads) and the oral primordium in opisthe (arrow). (**D**) To show new cirri derived from the frontal-ventral-transverse cirral anlagen. (**E**) Ventral view, arrows point to the paroral membrane (PM) in the proter and the development of the PM-anlage in the opisthe; arrowhead indicates the frontal cirrus I/1 in the opisthe formed *de novo*. (**F**) Ventral view, indicating the marginal anlagen of the proter (arrow) and the opisthe (arrowhead). (**G**) Arrowheads showing the dorsal kinety anlage of an early divider. (**H**) Portion of the ventral view, showing the marginal cirri in the proter (arrow) and the opisthe (arrowhead). (**I**) Dorsal view, arrowheads indicating the development of the dorsal kinety anlage. (**J**) Portion of the dorsal view, to show the newly formed caudal cirri in the proter (arrowheads). Scale bars: 100 μm.

pattern (Figs 3C, 4D), migrating to develop as distinct cirri to daughter cells.

Immediately following the breakup of the FVT-anlagen, two small patches of kinetosomes appear in the outermost region of the cortex near the original left-most frontal cirrus and between two adoral zone membranelles (Figs 3C, 4E). These patches form new anlage for the frontal cirrus I/1 of the proter and opisthe respectively. These two anlagen are formed *de novo*, i.e. evidently no old cirrus or paroral membrane is involved in the formation of the anlagen. Subsequently, these two anlagen develop into the frontal cirrus I/1 by rapid proliferation of kinetosomes and migrate to their final positions (Figs 3E, G).

Development of marginal cirri: the anlagen of the left marginal cirri for the proter and opisthe are formed *de novo*. One anlage for the marginal cirri forms as a short row of kinetosomes near the parental adoral zone in the proter, and the other near the newly formed adoral zone in the opisthe (Fig. 4F). Each anlage subsequently enlarges and segments to form the marginal cirri for daughter cells (Figs 3C, 4H).

Nuclear division: each end of the macronucleus has a recognizable replication band in the early stage (Fig. 3B). As the replication bands progress, the macronucleus changes shape to become a short strand after the process of replication of the nuclear apparatus (Figs 3D, F, 4A). As the daughter cells separate, the nodular macro-

nucleus divides to form the 3-shaped nucleus, both in the proter and the opisthe.

Development of dorsal ciliature: on the dorsal side, the proliferation of new basal bodies occurs in the midline of each parental dorsal kinety in a non-typical primary mode, i.e. dorsal kinety anlagen composed of densely arranged basal bodies are not formed (Fig. 4G). With further proliferation, these sparsely distributed anlagen break apart and develop into two groups of kinetal rows, moving anteriorly and posteriorly, eventually replacing the old structures (Figs 4I, J).

In the proter, two caudal cirri are formed at the posterior end of the right-most two dorsal kinety anlagen (Figs 3C, D, 4J). Meanwhile, in the opisthe, two caudal cirri are formed at the end of the right-most two dorsal kinety rows (Figs 3C, D, E, F).

SSU rRNA gene sequence and phylogenetic analyses (Fig. 5): The SSU rRNA gene sequence of *Euplotes amieti* was deposited in GenBank with accession number KJ524911. The length and GC content of the SSU rRNA gene (not including primers) were 1783 bp and 43.97%, respectively. Phylogenetic trees based on the SSU rRNA gene sequences were constructed using two different methods: Bayesian inference (BI) and maximum-likelihood (ML). The topologies of the BI and ML trees were almost identical and, for purposes of illustration, they were therefore merged into a single tree (Fig. 5).

We included a broad selection of all the SSU rRNA gene sequences of the order Euplotida from GenBank in the phylogenetic analyses. As shown in Fig. 5, the order Euplotida is composed of five families, namely Aspidiscidae, Certesiidae, Euplotidae, Gastrocirrhidae, and Uronychiidae. The Order Euplotida is monophyletic in all analyses.

All available SSU rRNA gene sequences of the *Euplotes*-complex were included in our phylogenetic analyses. The analyses provide full bootstrap support and posterior probability (PP) for the monophyly of Euplotidae (100% ML, 1.00 BI). As shown in Fig. 5, all *Euplotes*-complex species form a well-supported group with full posterior probability and bootstrap values (100% ML, 1.00 BI). This group includes six major clades designated according to Yi *et al*. (2009) based on morphological and phylogenetic information, although support for several of the nodes is rather low (Jiang *et al*. 2010) and the relationships of *Euplotes dammamensis* (JX185743), *Euplotes parabalteatus* (FJ346568) and *Euplotes sinicus* (FJ423448) remain unresolved.

We obtained all the SSU rRNA sequences from five isolates of *Euplotes eurystomus*. *Euplotes amieti* clusters with four isolates of *E. eurystomus* in Clade I with full support values (100% ML, 1.00 BI), apart from *Euplotes eurystomus* iso5 (AF452707), which groups with *E. aediculatus* (EU103618) in Clade I with maximum support.

DISCUSSION

Comparison of the Shanghai population of *Euplotes amieti* with other isolates: Since being originally reported by Dragesco (1970), this species has been redescribed on only two occasions (Dragesco 1972, 2003). The original population is larger (130–220 μm × 70–150 μm vs. 130–200 μm × 70–100 μm) and has slightly more dorsal kineties (14 vs. 13 on average) than our population, and there is a well-developed concave on the right side of the peristome, which is not very strong in our population of *Euplotes amieti*.

The Chadian population is 180 μm long in average (vs. 130–200 μm in Shanghai population), with about 13 dorsal kineties (vs. 12–14), which resembles the average number in the Shanghai population.

The population harvested in Rwanda in 1985 and redescribed by Dragesco (2003) has no living size data but only an average size of fixed or impregnated cells (169 μm in average length vs. 142 μm in the Shanghai population). The Rwandan population has slightly more dorsal kineties (12–15, 14 on average vs. 12–14, 13 on average) than the Shanghai population. It also has a conspicuous deep pocket on the right side of the peristome (vs. weak concave on the right side in our population).

Comparison of the Shanghai population of *Euplotes amieti* with four morphologically similar forms: Given the double-*eurystomus* type of dorsal silverline system and consistently nine frontoventral cirri, four morphologically similar forms should be compared with our population of *Euplotes amieti*, namely *Euplotes aediculatus* Pierson, 1943, *Euplotes eurystomus* Wrzesniowski, 1870, *Euplotes woodruffi* Gaw, 1939 and *Euplotes finki* Foissner, 1982 (shown in Table 2).

Of these species, *Euplotes eurystomus* is very similar to *Euplotes amieti* in terms of its infraciliature and the shape of the AZM and macronucleus. However, the former can be separated from the latter by its smaller

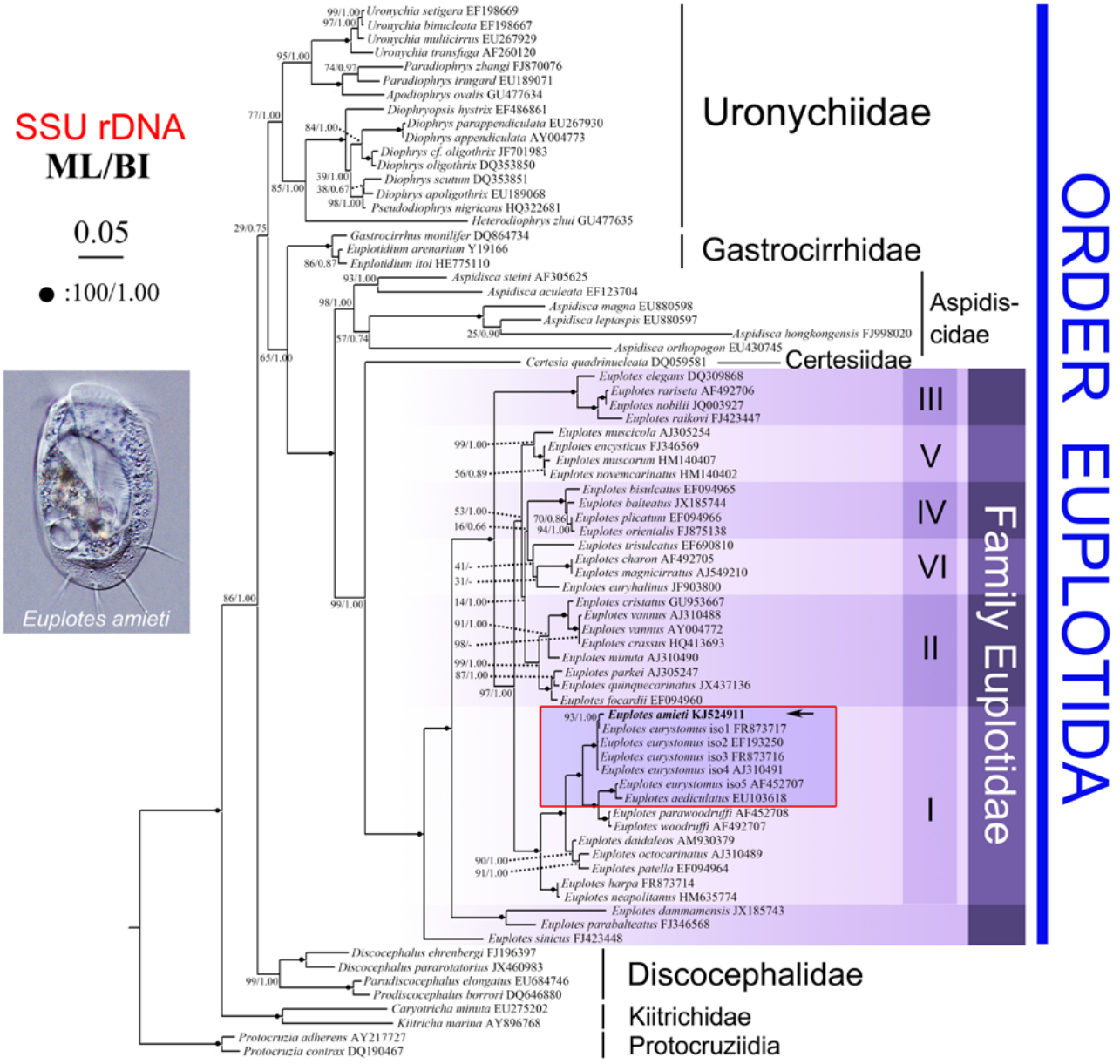

Fig. 5. Phylogenetic tree based on SSU rRNA gene sequences, showing the position of *Euplotes amieti* (arrow) by Maximum Likelihood (ML) and Bayesian inference (BI). Numbers near branches denote ML bootstrap value/BI posterior probability value. '–' indicates topologies that differ between the ML and BI phylogenies. Fully supported (100%/1.00) branches are marked with solid circles. All branches are drawn to scale. The scale bar corresponds to 5 substitutions per 100 nucleotide positions. GenBank accession numbers are given for each species. Systematic classification is mainly according to Lynn (2008). Euplotid clades I–VI were designated according to Yi *et al*. (2009).

body size (100–160 μm × 40–90 μm vs. 130–200 μm × 70–100 μm in *E. amieti*), its body shape (the posterior part is more rounded in *E. amieti*) and fewer dorsal kineties (eight to 12 vs. 12–14 in our population) (Curds 1975, Ma *et al*. 2000, Dragesco 2003).

Euplotes aediculatus differs from *Euplotes amieti* in having dorsal ridges (vs. no conspicuous dorsal ridges in *E. amieti*), fewer adoral membranelles (40–60, usually 50 vs. 60–65 in *E. amieti*), fewer dorsal kineties (eight, rarely nine vs. 12–14), fewer depressions in the

Table 2. Comparison of *Euplotes amieti* Dragesco, 1970 with those related congeners with a double-*eurystomus* type of dorsal silverline system and consistently nine frontoventral cirri.

Characteristic	E. amieti	E. amieti	E. eurystomus	E. aediculatus	E. woodruffi	E. finki
Cell size *in vivo* (μm)	130–200 × 70–100	140–240 × 80–160*	100–160 × 40–90	105–165 × 60–110	110–160 × 60–80	ca. 60 × 40
No. of AM	60–65	53–67	50–65	40–60	59–70	19–22
No. of DK ($\bar{x}$)	12–14 (13)	12–15 (14)	8–12 (10)	8, rarely 9	9–10	ca. 7
No. of dikinetids in mid-dorsal kinety	18–26	21–28	17–25	20**	ca. 22	ca. 10
Macronucleus	3-shaped	3-shaped	3-shaped	C- to inconspicuous 3-shaped	T- or Y-shaped	C- to J-shaped
Body features	Collar conspicuous, sigmoid AZM	Collar conspicuous, sigmoid AZM	Collar conspicuous, sigmoid AZM	Collar conspicuous, AZM straight to curved but never sigmoidal, having ridges on dorsal side	Collar conspicuous, AZM almost straight	Collar not conspicuous, AZM curving, conspicuous ridges on dorsal side
Data source	Original	Dragesco (2003)	Curds (1975)	Foissner (1991)	Dai *et al.* (2013)	Foissner (1982)

Abbreviations: AM, adoral membranelles; DK, dorsal kineties; $\bar{x}$, average value.
* Data from Dragesco, 1970.
** Data from Curds, 1975.

median border of the peristome (two vs. three or more in *E. amieti*), the shape of the AZM straight to curved but never sigmoidal (vs. definitely sigmoidal in *E. amieti*) and inverted C-shaped macronucleus that is slightly depressed on a flattened back (vs. 3-shaped in *E. amieti*) (Pierson *et al*. 1968, Augustin and Foissner 1989, Foissner *et al.* 1991, Pang and Wei 1999, Dragesco 2003).

Euplotes woodruffi resembles *Euplotes amieti* in cell size, length of buccal field, and the number of adoral membranelles and dikinetids in the mid-dorsal kinety; however, *Euplotes woodruffi* can be distinguished from *Euplotes amieti* by the shape of its macronucleus (T-shaped vs. 3-shaped in *E. amieti*) and AZM (almost straight in the ventral part vs. sigmoidal in *E. amieti*), as well as the number of dorsal kineties (nine to 10 vs. 12–14 in *E. amieti*) and grooves on the dorsal side (eight to 10 vs. no conspicuous groove in *E. amieti*). It is notable that *Euplotes woodruffi* has been isolated from both freshwater and low salinity estuaries (Song and Bradbury 1997, Dragesco 2003, Dai *et al*. 2013).

Euplotes finki can be easily separated from *Euplotes amieti* due to its smaller body size (60 μm × 40 μm vs. 130–200 μm × 70–100 μm in *E. amieti*), conspicuous ridges on the dorsal side (vs. no prominent ridges on dorsal side of *E. amieti*), numbers of dorsal kineties (seven vs. 12–14 in *E. amieti*) and dikinetids in the mid-dorsal kinety (ca. 10 vs. 21–24 in *E. amieti*), arrangement of transverse cirri (three right and two left transverse cirri separated by a remarkably wide space vs. five close-set transverse cirri in *E. amieti*), the shape of the macronucleus (C- to almost J-shaped vs. 3-shaped), no conspicuous collar zone (vs. prominent collar zone in *E. amieti*) and the shape of the AZM (curving vs. sigmoidal in *E. amieti*) (Foissner 1982, Dragesco 2003).

Phylogenetic analyses of *Euplotes amieti* and five isolates of *Euplotes eurystomus* based on SSU rRNA gene sequence data: The sequence of *Euplotes amieti* (KJ524911) differs in only 4–11 nucleotides from all the sequences of *Euplotes eurystomus* except *Euplotes eurystomus* iso5 (AF452707) (shown in Table 3). It is noteworthy that the newly sequenced *Euplotes amieti* (KJ524911) and *Euplotes eurystomus* iso1–4 grouped together with full support (100% ML, 1.00 BI). *Euplotes amieti* and *Euplotes eurystomus* are very similar in cell size, number of adoral membranelles, the shape of the adoral zone and macronucleus and in having a prominent collar. The most significant difference between *Euplotes amieti* and *Euplotes eurystomus* is the number of dorsal kineties, which can be detected only after protargol impregnation. Furthermore, no morphological information is available regarding *Euplotes eurystomus* iso1–4, so misidentification cannot be excluded, and accordingly these four sequences (FR873717, EF193250, FR873716 and AJ310491) should be considered carefully.

Table 3. Sequence dissimilarities between the SSU rRNA gene of *Euplotes amieti*, five isolates of *Euplotes eurystomus*, and *Euplotes aediculatus*, determined by BioEdit 7.0.5.2 (Hall 1999).

Species	1	2	3	4	5	6	7
1. *E.amieti*	–	99.7	99.6	99.4	99.3	96.4	96.1
2. *E.eurystomus* iso1	4	–	99.8	99.7	99.6	96.5	96.2
3. *E.eurystomus* iso2	7	3	–	99.8	99.7	96.5	96.3
4. *E.eurystomus* iso3	9	5	2	–	99.6	96.4	96.1
5. *E.eurystomus* iso4	11	7	4	6	–	96.4	96.1
6. *E.eurystomus* iso5	64	62	61	63	64	–	99.1
7. *E.aediculatus*	69	67	66	68	69	16	–

Values below the diagonal are numbers of different sites; those above the diagonal are sequence identification percentages.

The dissimilarities in SSU rRNA topology between *Euplotes amieti* (KJ524911) and *Euplotes eurystomus* iso5 (AF452707) are firmly supported by the SSU rRNA gene sequence data. The newly sequenced *Euplotes amieti* differs in 64 nucleotides from the sequence of *Euplotes eurystomus* iso5 (AF452707), while the latter differs in 16 nucleotides from *Euplotes aediculatus* (EU103618) (Table 3), which is in accordance with morphological classification. *Euplotes eurystomus* iso5 (AF452707) can be characterized as follows: body size 88–125 μm × 55–78 μm *in vivo*, about 48 membranelles on the sigmoidal AZM with a prominent collar; usually 9 dorsal kineties; a basically 3-shaped macronucleus and a 'double-*eurystomus*' type of silverline system. These characteristics match well with the original description of *Euplotes eurystomus* (Ma *et al.* 2000), so its identification is correct.

Acknowledgements. This work was supported by the Natural Science Foundation of China (project number: 31272285), and King Saud University Deanship for Scientific Research, Prolific Research Group (PRG-1436-01). Special thanks are due to Dr. Hong Zeng, Fujian Normal University, for kindly providing the materials. We gratefully acknowledge Prof. Weibo Song (OUC) for his helpful suggestions in drafting this paper. Many thanks are also due to Ms. Xiaolu Zhao and Dr. Feng Gao (OUC) for discussions during phylogenetic analysis; to Mr. Weibo Zheng and to Ms. Jie Huang (OUC) for their technical help.

REFERENCES

Achilles-Day U. E. M., Pröschold T., Day J. G. (2008) Phylogenetic position of the freshwater ciliate *Euplotes daidaleos* within the family of Euplotidae, obtained from small subunit rDNA gene sequence. *Denisia* **23:** 411–416

Augustin H., Foissner W. (1989) Morphologie einiger Ciliaten (Protozoa: Ciliophora) aus dem Belebtschlamm. *Lauterbornia* **1:** 38–59

Borror A. C., Hill B. F. (1995) The order Euplotida (Ciliophora): taxonomy, with division of *Euplotes* into several genera. *J. Eukaryot. Microbiol.* **42:** 457–466

Carter H. P. (1972) Infraciliature of eleven species of the genus *Euplotes*. *Trans. Am. Microsc. Soc.* **91:** 466–492

Chen X., Zhao Y., Al-Farraj S. A., Al-Quraishy S. A., El-Serehy H. A., Shao C., Al-Rasheid K. A. S. (2013) Taxonomic descriptions of two marine ciliates, *Euplotes dammamensis* n. sp. and *Euplotes balteatus* (Dujardin, 1841) Kahl, 1932 (Ciliophora, Spirotrichea, Euplotida), collected from the Arabian Gulf, Saudi Arabia. *Acta Protozool.* **52:** 73–89

Curds C. R. (1975) A guide to the species of the genus *Euplotes* (Hypotrichida, Ciliatea). *Bull. Br. Mus. Nat. Hist. (Zool.).* **28:** 3–61

Curds C. R., Wu I. C. H. (1983) A review of the Euplotidae (Hypotrichida, Ciliophora). *Bull. Br. Mus. Nat. Hist. (Zool.).* **44:** 191–247

Dai R., Xu K., He Y. (2013) Morphological, physiological, and molecular evidences suggest that *Euplotes parawoodruffi* is a junior synonym of *Euplotes woodruffi* (Ciliophora, Euplotida). *J. Eukaryot. Microbiol.* **60:** 70–78

Dragesco J. (1970) Ciliés libres du Cameroun. *Ann. Fac. Sci. Jaoundé* (Hors série), 1–141

Dragesco J. (1972) Ciliés libres de l'Ouganda. *Ann. Fac. Sci. Univ. Féd. Cameroun* **9:** 87–126

Dragesco J. (2003) Infraciliature et morphometrie de vingt espèces de ciliés hypotriches recoltés au Rwanda et Burundi, comprenant *kahliella quadrinucleata* n. sp., *pleurotricha multinucleata* n. sp. et *laurentiella bergeri* n. sp. *Trav. Mus. Nat. d'Hist. Nat.* **45:** 7–59

Dragesco J., Dragesco-Kernéis A. (1986) Ciliés libres de l'Afrique intertropicale. Introduction à la connaissance et à l'étude des ciliés. *Faune Tropicale* **26:** 495–497

Edgar R. C. (2004) MUSCLE: multiple sequence alignment with high accuracy and high throughput. *Nucleic Acids Res.* **32:** 1792–1797

Fan Y., Chen X., Hu X., Shao C., Al-Rasheid K. A. S., Al-Farraj S. A., Lin X. (2014) Morphology and morphogenesis of *Apoholosticha sinica* n. g., n. sp. (Ciliophora, Hypotrichia), with consideration of its systematic position among urostylids. *Eur. J. Protistol.* **50:** 78–88

Foissner W. (1982) Ecology and taxonomy of the Hypotrichida (Protozoa: Ciliophora) of some Austrian soils. *Arch. Protistenkd.* **126:** 19–143

Foissner W. (2014) An update of 'basic light and scanning electron microscopic methods for taxonomic studies of ciliated protozoa'. *Int. J. Syst. Evol. Microbiol.* **64:** 271–292

Foissner W., Blatterer H., Berger H., Kohmann F. (1991) Taxonomische und ökologische Revision der Ciliaten des Saprobiensystems – Band I: Cyrtophorida, Oligotrichida, Hypotrichia, Colpodea. Informationsberichte des Bayer, Landesamtes für Wasserwirtschaft, München, **1/91:** 1–478

Gates M. A., Curds C. R. (1979) The dargyrome of the genus *Euplotes*. *Bull. Br. Mus. Nat. Hist. (Zool)*. **35:** 127–200

Hall T. A. (1999) BioEdit: a user-friendly biological sequence alignment editor and analysis program for Windows 95/98/NT. *Nucleic Acids Symp. Ser.* **41:** 95–98

Huang J., Dunthorn M., Song W. (2012) Expanding character sampling for the molecular phylogeny of euplotid ciliates (Protozoa, Ciliophora) using three markers, with a focus on the family Uronychiidae. *Mol. Phylogent. Evol.* **63:** 598–605

Huang J., Chen Z., Song W., Berger H. (2014) Three-gene based phylogeny of the Urostyloidea (Protista, Ciliophora, Hypotricha), with notes on classification of some core taxa. *Mol. Phylogent. Evol.* **70:** 337–347

Jiang J., Huang J., Li J., Al-Rasheid K. A. S., Al-Farraj S. A., Lin X., Hu X. (2013) Morphology of two marine euplotids (Ciliophora: Euplotida), *Aspidisca fusca* Kahl, 1928 and *A. hexeris* Quennerstedt, 1869, with notes on their small subunit rRNA gene sequences. *Eur. J. Protistol.* **49:** 634–643

Jiang J., Zhang Q., Warren A., Al-Rasheid K. A. S., Song W. (2010) Morphology and SSU rRNA gene-based phylogeny of two marine *Euplotes* species, *E. orientalis* spec. nov. and *E. raikovi* Agamaliev, 1966 (Ciliophora, Euplotida). *Eur. J. Protistol.* **46:** 121–132

Lynn D. H. (2008) The ciliated protozoa: characterization, classification and guide to the literature. 3rd ed. Springer Press, Dordrecht

Ma H., Gong J., Wang Y., Hu X., Ma H., Song W. (2000) Morphological studies on *Euplotes eurystomus* (Ciliophora, Hypotrichida) compared with its related species from freshwater biotopes. *J. Zibo Univ. (Nat. Sci. and Eng. Ed.)* **2:** 75–77 (in Chinese with English abstract)

Medlin L., Elwood H. J., Stickel S., Sogin M. L. (1988) The characterization of enzymatically amplified eukaryotes 16S-like ribosomal RNA coding regions. *Gene* **71:** 491–500

Nylander J. A. A. (2004) MrModeltest version 2. Program distributed by the author. Department of Systematic Zoology, Evolutionary Biology Centre, Uppsala University, Uppsala

Page R. D. M. (1996) TREEVIEW: an application to view phylogenetic trees on personal computers. *Comput. Appl. Biosci.* **12:** 357–358

Pan Y., Li L., Shao C., Hu X., Ma H., Al-Rasheid K. A. S., Warren A. (2012) Morphology and ontogenesis of a marine ciliate, *Euplotes balteatus* (Dujardin, 1841) Kahl, 1932 (Ciliophora, Euplotida) and definition of *Euplotes wilberti* nov. spec. *Acta Protozool.* **51:** 29–38

Pang Y., Wei H. (1999) Studies on the Morphology and Morphogenesis in *Euplotes aediculatus*. *J. East China Normal Univ. (Natural Science)* **1:** 103–109 (in Chinese with English abstract)

Petroni G., Dini F., Verni F., Rosati G. (2002) A molecular approach to the tangled intrageneric relationships underlying phylogeny in *Euplotes* (Ciliophora, Spirotrichea). *Mol. Phylogenet. Evol.* **22:** 118–130

Pfeiffer W., Stamatakis A. (2010) Hybrid parallelization of the MrBayes and RAxML phylogenetics codes.

Pierson D. M., Kimball R. F., Carrier R. F. (1968) Clarification of the taxonomic identification of *Euplotes eurystomus* Kahl and *E. aediculatus* Pierson. *Trans. Am. Microsc. Soc.* **72:** 125–151

Posada D., Crandall K. A. (1998) Modeltest: testing the model of DNA substitution. *Bioinformatics* **14:** 817–818

Pratas F., Trancoso P., Stamatakis A., Sousa L. (2009) Fine-grain parallelism using Multi-core, Cell/BE, and GPU systems: accelerating the phylogenetic likelihood function. Proceedings of ICPP Vienna, Austria.

Ronquist F., Huelsenbeck J. P. (2003) MRBAYES 3: Bayesian phylogenetic inference under mixed models. *Bioinformatics* **19:** 1572–1574

Schwarz M., Zuendorf A., Stoeck T. (2007) Morphology, ultrastructure, molecular phylogeny, and autecology of *Euplotes elegans* Kahl, 1932 (Hypotrichida; Euplotidae) isolated from the Anoxic Mariager Fjord. Denmark. *J. Eukaryot. Microbiol.* **54:** 125–136

Shao C., Ding Y., Al-Rasheid K. A. S., Al-Farraj S. A., Warren A., Song W. (2013a) Establishment of a new hypotrichous genus, *Heterotachysoma* n. gen. and notes on the morphogenesis of *Hemigastrostyla enigmatica* (Ciliophora, Hypotrichia). *Eur. J. Protistol.* **49:** 93–105

Shao C., Pan X., Jiang J., Ma H., Al-Rasheid K. A. S., Warren A., Lin X. (2013b) A redescription of the oxytrichid *Tetmemena pustulata* (Müller, 1786) Eigner, 1999 and notes on morphogenesis in the marine urostylid *Metaurostylopsis salina* Lei *et al*., 2005 (Ciliophora, Hypotrichia). *Eur. J. Protistol.* **49:** 272–282

Song W., Bradbury P. (1997) Comparative studies on a new brackish water *Euplotes*, *E. parawoodruffi* n. sp., and a redescription of *Euplotes woodruffi* GAW, 1939 (Ciliophora; Hypotrichida). *Arch. Protistenkd.* **148:** 399–412

Song W., Warren A., Hu X. (2009) Free-living ciliates in the Bohai and Yellow Seas, China. Science Press, Beijing

Stamatakis A. (2006) RAxML-VI-HPC: Maximum likelihood-based phylogenetic analyses with thousands of taxa and mixed models. *Bioinformatics* **22:** 2688–2690

Stamatakis A., Hoover P., Rougemont J. (2008) A fast bootstrapping algorithm for the RAxML web-servers. *Syst. Biol.* **57:** 758–771

Tamura K., Dudley J., Nei M., Kumar S. (2007) MEGA 4: molecular evolutionary genetics analysis (MEGA) software Ver. 4.0. *Mol. Biol. Evol.* **24:** 1596–1599

Tuffrau M. (1960) Révision du genre *Euplotes*, fondée sur la comparaison des structures superficielles. *Hydrobiologia* **15:** 1–77

Wilbert N. (1975) Eine verbesserte Technik der Protargolimprägnation für Ciliaten. *Mikrokosmos* **64:** 171–179

Yi Z., Song W., Clamp J., Chen Z., Gao S., Zhang Q. (2009) Reconsideration of systematic relationships within the order Euplotida (Protista, Ciliophora) using new sequences of the gene coding for small-subunit rRNA and testing the use of combined data sets to construct phylogenies of the *Diophrys*-like species. *Mol. Phylogent. Evol.* **50:** 599–607

Yi Z., Katz L. A., Song W. (2012) Assessing whether alpha-tubulin sequences are suitable for phylogenetic reconstruction of Ciliophora with insights into its evolution in euplotids. *PLoS ONE* **7:** e40635. doi:10.1371/journal.pone.0040635

Received on 22nd May, 2014; revised on 5th October, 2014; accepted on 16th October, 2014